SINTEF
PROCEEDINGS
2

Proceedings of the 12th International Conference on Computational Fluid Dynamics in the Oil & Gas, Metallurgical and Process Industries

Progress in Applied CFD – CFD2017

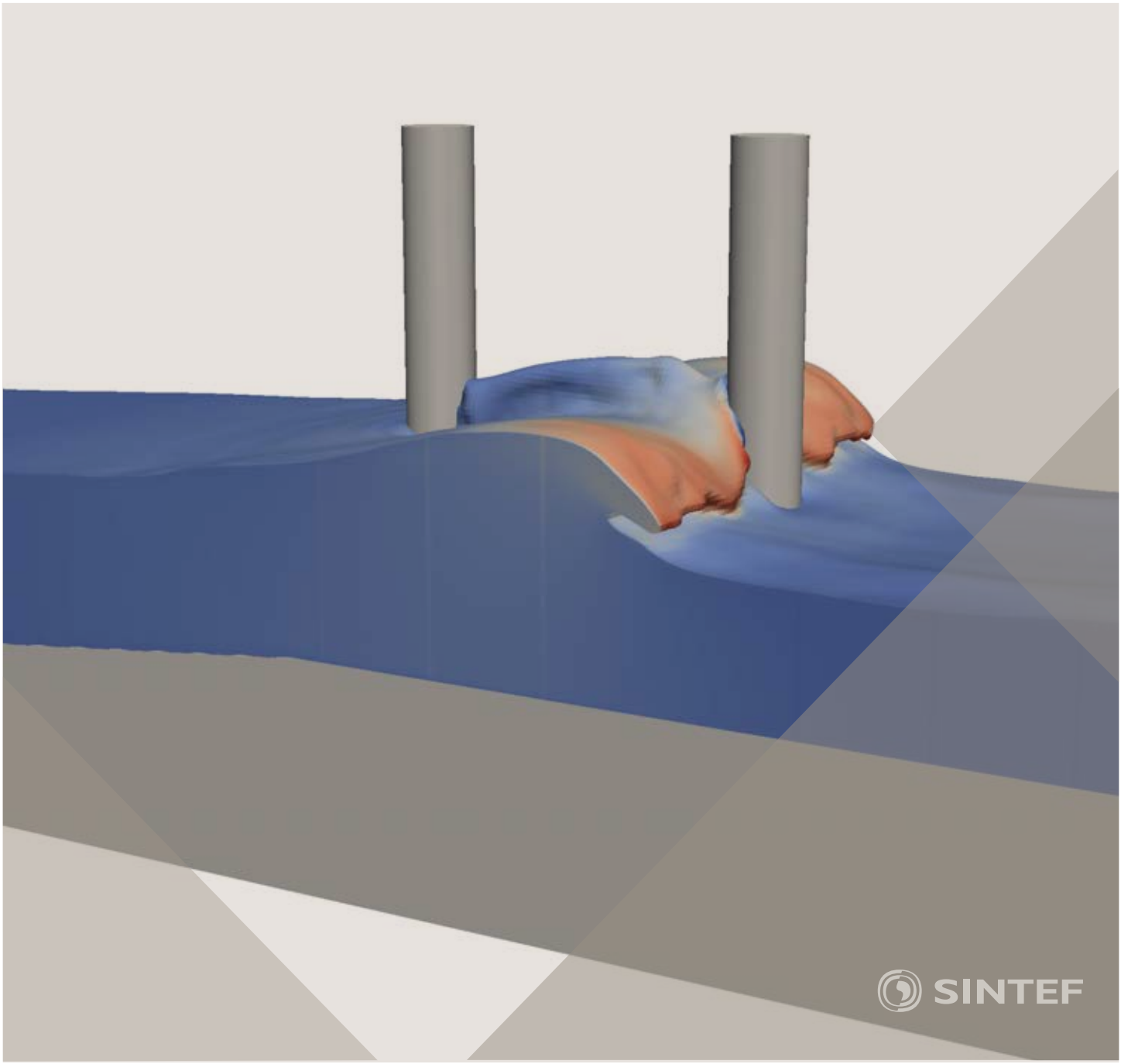

SINTEF Proceedings

Editors:
Jan Erik Olsen and Stein Tore Johansen

Progress in Applied CFD – CFD2017

Proceedings of the 12th International Conference on Computational Fluid Dynamics in the Oil & Gas, Metallurgical and Process Industries

SINTEF Academic Press

SINTEF Proceedings no 2
Editors: Jan Erik Olsen and Stein Tore Johansen
Progress in Applied CFD – CFD2017
Selected papers from 10th International Conference on Computational Fluid Dynamics in the Oil & Gas, Metallurgical and Process Industries

Key words:
CFD, Flow, Modelling

Cover, illustration: Arun Kamath

ISSN 2387-4295 (online)
ISBN 978-82-536-1544-8 (pdf)

SINTEF Academic Press
Address: Forskningsveien 3 B
PO Box 124 Blindern
N-0314 OSLO
Tel: +47 73 59 30 00
Fax: +47 22 96 55 08

www.sintef.no/byggforsk
www.sintefbok.no

SINTEF Proceedings
SINTEF Proceedings is a serial publication for peer-reviewed conference proceedings on a variety of scientific topics.
The processes of peer-reviewing of papers published in SINTEF Proceedings are administered by the conference organizers and proceedings editors. Detailed procedures will vary according to custom and practice in each scientific community.

PREFACE

This book contains all manuscripts approved by the reviewers and the organizing committee of the 12th International Conference on Computational Fluid Dynamics in the Oil & Gas, Metallurgical and Process Industries. The conference was hosted by SINTEF in Trondheim in May/June 2017 and is also known as CFD2017 for short. The conference series was initiated by CSIRO and Phil Schwarz in 1997. So far the conference has been alternating between CSIRO in Melbourne and SINTEF in Trondheim. The conferences focuses on the application of CFD in the oil and gas industries, metal production, mineral processing, power generation, chemicals and other process industries. In addition pragmatic modelling concepts and bio-mechanical applications have become an important part of the conference. The papers in this book demonstrate the current progress in applied CFD.

The conference papers undergo a review process involving two experts. Only papers accepted by the reviewers are included in the proceedings. 108 contributions were presented at the conference together with six keynote presentations. A majority of these contributions are presented by their manuscript in this collection (a few were granted to present without an accompanying manuscript).

The organizing committee would like to thank everyone who has helped with review of manuscripts, all those who helped to promote the conference and all authors who have submitted scientific contributions. We are also grateful for the support from the conference sponsors: ANSYS, SFI Metal Production and NanoSim.

Stein Tore Johansen & Jan Erik Olsen

Organizing committee:

Conference chairman: Prof. Stein Tore Johansen
Conference coordinator: Dr. Jan Erik Olsen
Dr. Bernhard Müller
Dr.Sigrid Karstad Dahl
Dr.Shahriar Amini
Dr.Ernst Meese
Dr.Josip Zoric
Dr.Jannike Solsvik
Dr.Peter Witt

Scientific committee:

Stein Tore Johansen, SINTEF/NTNU
Bernhard Müller, NTNU
Phil Schwarz, CSIRO
Akio Tomiyama, Kobe University
Hans Kuipers, Eindhoven University of Technology
Jinghai Li, Chinese Academy of Science
Markus Braun, Ansys
Simon Lo, CD-adapco
Patrick Segers, Universiteit Gent
Jiyuan Tu, RMIT
Jos Derksen, University of Aberdeen
Dmitry Eskin, Schlumberger-Doll Research
Pär Jönsson, KTH
Stefan Pirker, Johannes Kepler University
Josip Zoric, SINTEF

CONTENTS

TIRE RUBBER EXTRUDATE SWELL SIMULATION AND VERIFICATION WITH EXPERIMENTS

J Buist, DJ Van Dijk, TJ Mateboer*

Windesheim University Professorship for Polymer Engineering, 8000 GB Zwolle, the Netherlands

* E-mail: t.j.mateboer@windesheim.nl

ABSTRACT

Extrudate swell simulations and experiments have been performed with a viscoelastic tire rubber compound at high flow rates through a circular die. A 3-mode PTT model was fitted onto rheological data of the rubber. The PTT model covers the range of shear rates present in the simulation. Convergence of the simulation was achieved with some wall slippage. The simulated and experimental extrudate swell is in good agreement at 20 mm from the die exit for a wide range of flow rates.

Keywords: CFD, extrudate swell, die swell, PTT, viscoelasticity, tire rubber compound

NOMENCLATURE

Greek Symbols

$\dot{\gamma}$	Shear rate, [s^{-1}].
ε	Strain (elasticity) parameter of the PTT model, [-].
ξ	Slip parameter of PTT model, [-] [1].
η^*	Dynamic viscosity, [Pa·s].
η	Viscosity, [Pa·s].
λ	relaxation time, [s].
ρ	Mass density, [$kg \cdot m^{-3}$].
σ_n	Stress normal to plane direction, [Pa].
τ_{wall}	The shear stress at the wall, [Pa].
ω	Oscillation frequency, [$rad \cdot s^{-1}$].

Latin Symbols

H	Diameter of the extrudate, [m].
H_0	Diameter of the die, [m].
$\boldsymbol{D}$	Rate of deformation tensor, [s^{-1}].
$\boldsymbol{g}$	Gravity field, [$m \cdot s^{-2}$].
G'	Storage modulus, [Pa].
G''	Loss modulus, [Pa].
k	Slip coefficient, [$kg \cdot m^{-2} \cdot s^{-1}$].
m_{η^*}	Power law coefficient, [$Pa \cdot s^{n_{\eta^*}} \cdot Rad^{1-n_{\eta^*}}$].
$m_{G'}$	Power law coefficient, [$Pa \cdot s^{n_{G'}-1} \cdot Rad^{1-n_{G'}}$].
n_{η^*}	power law index, [-].
$n_{G'}$	power law index, [-].
p	Pressure, [Pa].
Q	Flow rate, [$m^3 \cdot s^{-1}$].
r	Viscosity ratio, [-].
rpm	Rotations per minute of the gear pump.
S	Swell ratio, [-].
t	Time, [s].
T_g	glass-liquid transition temperature, [°C]
$\boldsymbol{T}$	Stress tensor, [Pa].
$\overset{\Delta}{\boldsymbol{T}}_1$	Upper-convected derivative of tensor $\boldsymbol{T}$, [Pa].
$\overset{\nabla}{\boldsymbol{T}}_1$	Lower-convected derivative of tensor $\boldsymbol{T}$, [Pa].
$\boldsymbol{v}$	Velocity field, [m/s].
v_s	Velocity at the wall, the slip velocity, [$m \cdot s^{-1}$]

INTRODUCTION

Unvulcanized rubber extrusion is a key process in the tire industry. When rubber is extruded the extrudate will swell, a phenomenon called ‘extrudate swell’ or ‘die swell’. The degree of extrudate swell is dependent on many process parameters, among those parameters are the die shape, production rate, rubber composition and the elastic behavior of the rubber. Extrusion die design is a costly and time consuming process due to extrudate swell. Die design may be aided by numerical simulations of the extrusion process [2]. Flow patterns and pressure build up (flow resistance) within the die may be simulated with standard (fluid mechanics) numerical methods. However, extrudate swell poses specific problems because of the viscoelastic nature of the material, and because of the complex boundary conditions. There seems to be a growing interest in the tire making industry in simulating the extrusion of tire rubber [3-8]. This study proposes a procedure for aiding die design for industrial rubber extrusion by performing rheological measurements and numerical simulations. The simulated extrudate swell is verified with experimental extrudate swell.

Theory

Extrudate swell is a complex phenomenon. There are several contributing factors identified [9]. Swelling due to rearrangement of the velocity field, which happens in Newtonian fluids and Non-Newtonian fluids alike. This is only a small contribution for viscoelastic fluids like

rubber. The main cause of extrudate swell in viscoelastic fluids is elastic recovery.
It is unlikely that an analytical solution can be found to calculate extrudate swell according to R. I. Tanner [9]. This is due to the stress singularity which occurs at the change of boundary conditions from zero velocity at the die wall into the free-surface.

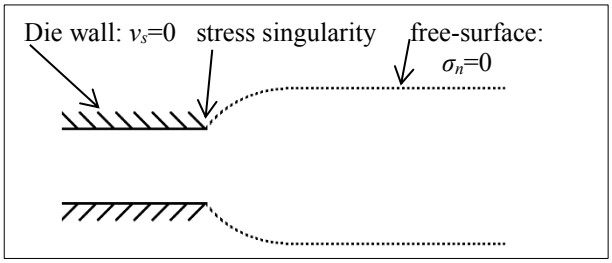

Figure 1: Schematic representation of extrudate swell. Velocities are zero at the die wall. At the free-surface the stresses normal to the free surface are zero [9].

Locating the free-surface is difficult. For this reason many attempts to calculate extrudate swell involve numerical methods. These methods need constitutive equations to describe the behavior of viscoelastic materials. Examples of viscoelastic models often applied in extrudate swell simulation studies are:

- Kaye-Bernstein-Kearsley-Zapas model [10-14]
- Pom-Pom model [14-17]
- Algebraic Extra-Stress Model [16, 18-20]
- Phan Thien & Tanner (PTT) model [8, 14-16, 20-30]

J.H. Kim and M.Y. Lyu have performed extrudate swell simulations with several viscoelastic models [16]. The PTT model shows good agreement with capillary rheometer experiments. Therefore the PTT model is applied in this study. Extrudate swell simulation studies are often conducted at relatively low flow rates and low shear rates [8, 14, 15, 31]. But in industrial rubber extrusion processes high flow rates and shear rates occur. This study is focused on extrudate swell at industrial flow rates.

EXPERIMENTAL SETUP

Extrusion experiments

Apollo tyres provided a rubber compound suitable for tire production. VMI Group performed several extrudate swell experiments. The rubber was extruded with a Shark 70 extruder, the shape and dimensions of the extrudate swell was captured on camera from above the extrudate.

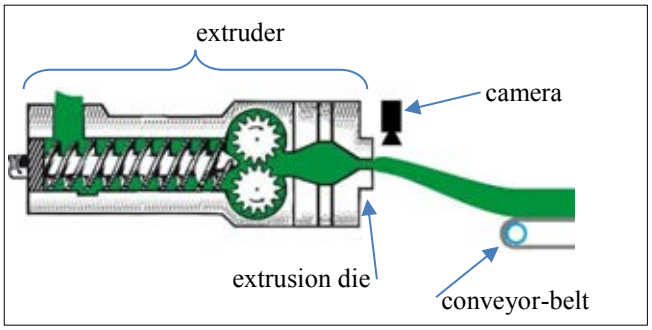

Figure 2: Schematic diagram of extrudate swell measurement setup.

The extrusion die is circular symmetrical and consist of a conical part and a capillary part.

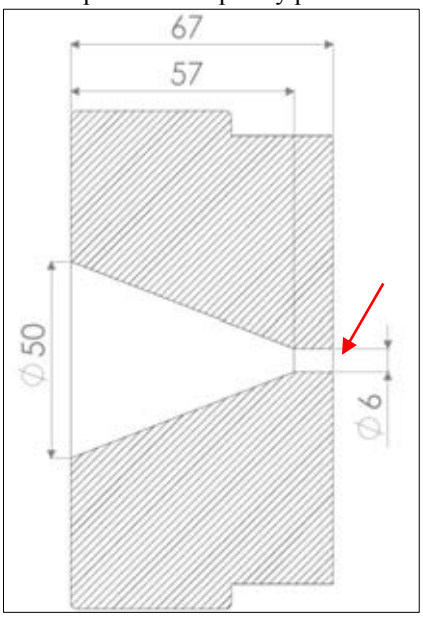

Figure 3: Cross-section of the circular symmetrical extrusion die, all dimensions are in mm. The rubber flow direction is from left to right. The red arrow points were the rubber exits the die.

A conveyor belt transported the rubber away from the extruder. The conveyor-belt speed was visually matched to the extrudate velocity to avoid pulling on the rubber extrudate. Pulling on the rubber decreases the extrudate swell. Camera imaging was used to measure the extrudate swell at several distances from the die exit. The rubber curves downward upon exiting the die since the conveyor-belt is positioned lower than the die exit, see Figure 4. This results in lower accuracy measurements of the extrudate swell at greater distances from the die exit.

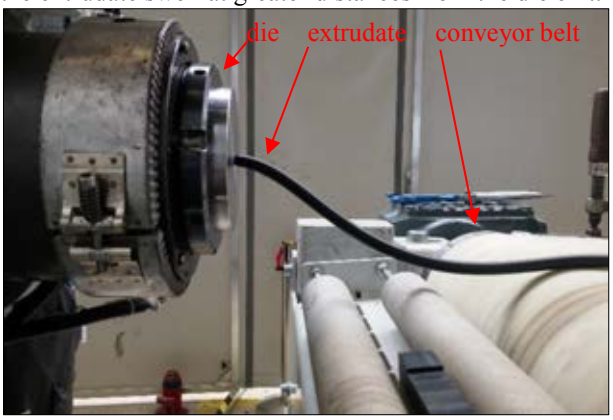

Figure 4: Photograph of the die, extruded rubber and conveyor belt, the camera is not included in this photograph.

The Shark 70 extruder consists of a conveying screw extruder and a gear-pump. The conveying screw extruder was set to produce a pressure of 30 Bar. Experiments have been performed at 4 different gear-pump speeds.

Table 1: Set gear-pump speeds and corresponding flow rates.

Gear pump speed	Flow rate
5 rpm	14.7 ml·s^{-1}
10 rpm	29.3 ml·s^{-1}
15 rpm	44.7 ml·s^{-1}
20 rpm	58.7 ml·s^{-1}

The flow rate was verified measuring the mass of extrudate collected during 36 s of extrusion. With each experiment, the temperature was measured at the inside of the extrudate. Extrudate swell (S) is expressed as the ratio of the diameter of the die and the extrudate diameter:

$$S = \frac{H - H_0}{H_0} \qquad 1$$

Rheological measurement setup

The G', G'' and η^* of the rubber compound were measured with an RPA2000 provided by the University of Twente. The RPA2000 is a cone-cone oscillatory rheometer. The cone geometry ensures that the shear rate is independent of the distance to the center of the cone.

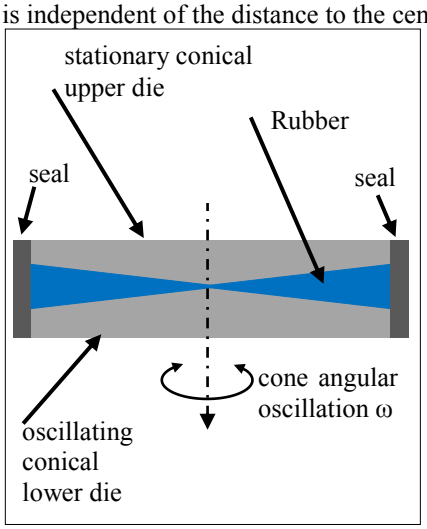

Figure 5: Schematic representation of the RPA2000, the conical dies are filled with a rubber specimen [32].

A rubber sample was subjected to a series of 9 measurements with a logarithmically increasing oscillation frequency of 0.07 rad·s^{-1} up to 209 rad·s^{-1}. Measurements with the RPA2000 were performed at 90 °C, 100 °C and 110 °C. The shear viscosity is calculated from the dynamic viscosity with the Cox-Merz rule [33].

$$\eta(\dot{\gamma}) = |\eta^*(\omega)|; \text{ with } \dot{\gamma} = \omega \qquad 2$$

SIMULATION SETUP

Constitutive model

The numerical simulations have been performed with Polyflow of the Ansys 17.2 simulation suite. Polyflow is FEM software which is often used for viscoelastic extrusion simulations [8, 10, 13, 14, 16, 17, 20, 31, 34-36]. Polyflow calculates the extra stress tensor of the momentum conservation equation (**3**) with equation 4 [37].

$$\rho\left(\frac{\partial \boldsymbol{v}}{\partial t} + \nabla \cdot (\boldsymbol{vv})\right) = -\nabla p + \nabla \boldsymbol{T} + \rho \boldsymbol{g} \qquad 3$$

$$\boldsymbol{T} = \boldsymbol{T}_1 + \boldsymbol{T}_2 \qquad 4$$

$\boldsymbol{T}_2$ is a purely viscous component which improves the convergence of the numerical method [37].

$$\boldsymbol{T}_2 = 2\eta \frac{r}{1-r}\boldsymbol{D} \qquad 5$$

$\boldsymbol{T}_1$ is calculated with the PTT viscoelastic model, equation 6 [37].

$$e^{\left[\frac{\varepsilon\lambda}{\eta}\mathrm{tr}(\boldsymbol{T}_1)\right]}\boldsymbol{T}_1 + \lambda\left[\left(1-\frac{\xi}{2}\right)\overset{\nabla}{\boldsymbol{T}}_1 + \frac{\xi}{2}\overset{\Delta}{\boldsymbol{T}}_1\right] = 2\eta\boldsymbol{D} \qquad 6$$

When a multi-mode viscoelastic model is used, the total extra stress tensor is the sum of the individual viscoelastic components. In order to limit the computational costs only 3 modes have been used.

All the simulations are isothermal. The finite element method is used for solving the system of equations, which involves a combination of the discrete elastic viscous stress splitting (DEVSS) and the streamline upwind (SU) method [37].

Curve fitting the PTT model parameters onto rheological data

The PTT model has several material specific parameters. The values of these parameters are found by fitting the PTT model onto the rheological data with Polymat. Polymat is an application for curve fitting and is available in Ansys 17.2. r, η, ε and ξ are fitted onto the measured G' and G''. ε and ξ are chosen to be identical for each PTT mode. The relaxation mechanism occurs near $1/\dot{\gamma}$ [37]. The relaxation times are not curve fitted but set as the reciprocal of the typical shear rates of the simulation. These typical shear rates were determined with a trial simulation. The trial simulation is similar to the extrudate swell simulation. To limit computational costs, the extrudate and the free surface were not included in the trial simulation. A trial multimode PTT model with very high and a very short relaxation times was used, all the other parameters were curve fitted onto the measured data. The trial simulation shows that typical shear rates are between 1 s^{-1} and 2000 s^{-1}. In the final multimode PTT model the relaxation times were chosen as 0.667 ms, 0.02 s and 0.6 s, which correspond with the typical shear rates of the trial simulation. The simulations with the final multimode PTT model do not exceed shear rates of 2130 s^{-1}.

Extrapolation of the measured data

Measurements with the RPA2000 are limited to 208 Rad·s^{-1} at a maximum. The typical shear rates of the simulation were much higher, therefore the measured η^*, G' and G'' were extrapolated in order to curve fit up to 1500 Rad·s^{-1}. With many rubber compounds a shear thinning effect is measured up to very high shear rates [38-40]. It is assumed that a power law is applicable with shear rates up to 1500 s^{-1}. Complex viscosity measurements are extrapolated using a power law which is fitted onto the rheological data. For G' an exponential relation was found. Finally G" is calculated with the extrapolated η^* and G'.

$$\eta^* = m_{\eta^*} \cdot \omega^{n_{\eta^*}-1} \qquad 7$$

$$G' = m_{G'} \cdot \omega^{n_{G'}} \qquad 8$$

$$G'' = \sqrt{\omega^2 \cdot \eta^{*2} - G'^2} \qquad 9$$

Boundary conditions

It was assumed that there is no wall slippage in the extrusion experiments, but the simulation would not converge without a certain amount of slippage at the die wall. This is most likely due to the high Weissenberg number problem. The high shear rates mostly occur near the die exit. Wall slippage was introduced in the extrudate swell simulations in order to temper the shear rates at the die exit. The wall slippage is enforced with equation 10 [37, 40].

$$v_s = -\frac{\tau_{wall}}{k} \qquad 10$$

There is a full-slip condition when k=0 kg·m^{-2}·s^{-1}, there is no slip if k=∞ kg·m^{-2}·s^{-1}. Wall slippage decreases the pressure drop in the die. The pressure drop can be expressed as a function of slip coefficient k. It was decided that a simulation performs sufficiently if the pressure drop is not significantly influenced by the wall slippage.

A simplified simulation was performed in order to find the pressure drop within the die. The simplified simulation is without extrudate and free surface, the simulation does converge without wall slippage. The simplified simulation was subsequently subjected to an incrementally increasing wall slippage. At k=10^8 kg·m^{-2}·s^{-1} the pressure drop became more than 95 % of that of the simulation without wall slippage. The extrudate swell simulations were performed with a wall slippage with a slip coefficient k=10^8 kg·m^{-2}·s^{-1}.

Finally, the surface of the extrudate is a free surface and the remeshing technique Optimesh-3D was applied [37]. At the outflow plane, a zero tangential and normal force condition was applied. This condition is applicable if the elastic tensions are completely dissipated.

Mesh

Several 3D meshes of the die and 40 mm of extrudate were designed. Some design consideration are:

- High node density near the die exit is desirable since the greatest increase in extrudate diameter is expected to happen near the die exit.
- Practice shows that a structured mesh of hexagonal cells results in a more stable simulation than an unstructured mesh.
- The computational costs increases rapidly with an increase in the number of nodes.
- Sufficient node density near the die wall since the shear rates are greatest near the die wall.

Figure 6 shows the cross-section through the length of the die and extrudate, the node density is higher near the die exit.

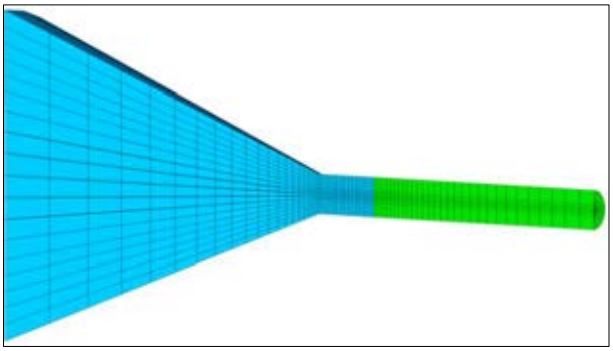

Figure 6: A cross-section through the length of the die and extrudate. Blue is the rubber inside the die, green is extrudate with a free surface. Note the higher node density near the die exit and larger cells further away from the die exit.

Simulations with several meshes were performed in order to find a mesh with a sufficient node density near the die wall. The node density near the die wall was determined by one variable, all other design parameters are kept constant, see Figure 7.

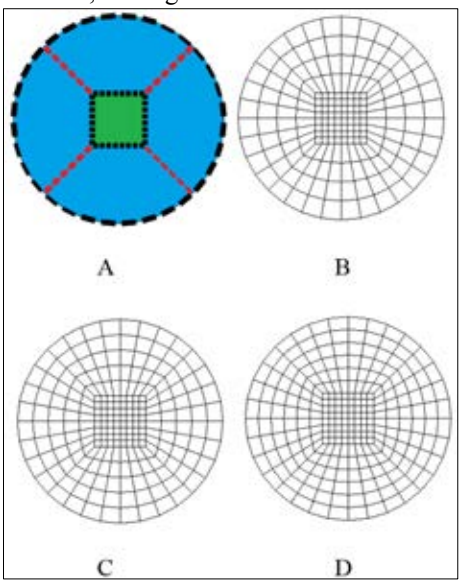

Figure 7: Width cross-sections of the meshes. A: Schematic representation of the mesh designs, the mesh consists of a square mid-section (green) and a circular part (blue). The total number of nodes is determined by a constant number of nodes in the angular direction (black) and a variable number of nodes in the radial direction (red). B: Cross-section of a mesh with 4 nodes in the radial direction. C: Cross-section of a mesh with 5 nodes in the radial direction. D: Cross-section of a mesh with 6 nodes in the radial direction.

A mesh is sufficient if the extrudate does not increase much when the number of nodes increases. The diameter of the extrudate at 20 mm from the die exit as a function of the number of nodes is shown in Figure 8.

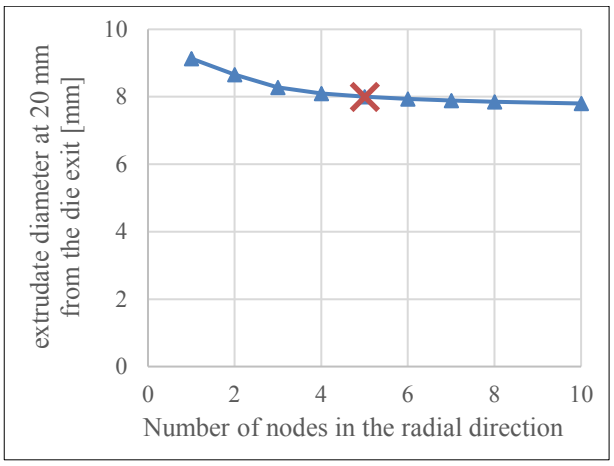

Figure 8: The extrudate diameter at 20 mm from the die exit as a function of the number of nodes in the radial direction with an flow rate of 13.9 ml·s^{-1}. The red cross at 5 nodes in the radial direction, this is the mesh used for the extrudate swell simulations.

The mesh used in this study is with 5 nodes in the radial direction. The mesh is structured with hexagonal cells and contains 15906 cells.

RESULTS AND DISCUSSION

Rheological measurements and curve-fit

The G', G'' and η were measured with the RPA2000, the rubber compound did not show a significant temperature dependence within the measured temperature range. This temperature independent behavior is expected since the rubber compound has a low T_g of less than 0 °C. The measurements at 100 °C have been used for extrapolation and curve-fitting. The measured G', G'' and η and the extrapolated data is shown in Figure 9.

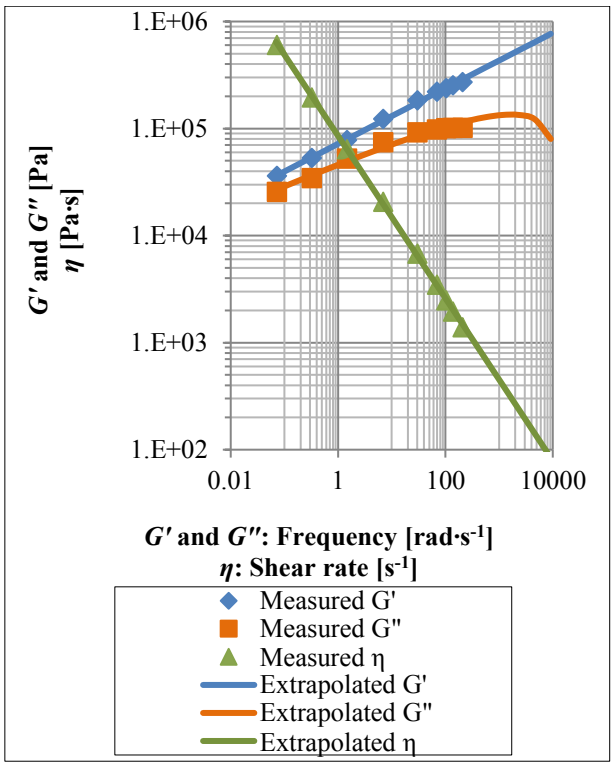

Figure 9: Measured and extrapolated G', G'' and η. Note: the dimensions differ between G', G'' and η. Note: all dimensions are presented on a logarithmic scale.

Equations 7, 8 and 9 are applied for the extrapolation of G', η and G''. The following values for the parameters of these equations were found:

- $m_{\eta^*} = 85422$ Pa·s$^{n_{\eta^*}}$·Rad$^{1-n_{\eta^*}}$
- $n_{\eta^*} = 0.241$
- $m_{G'} = 72078$ Pa·s$^{n_{G'}}$·Rad$^{-n_{G'}}$
- $n_{G'} = 0.259$

A curve fit was made onto the extrapolated data and is shown in Figure 10.

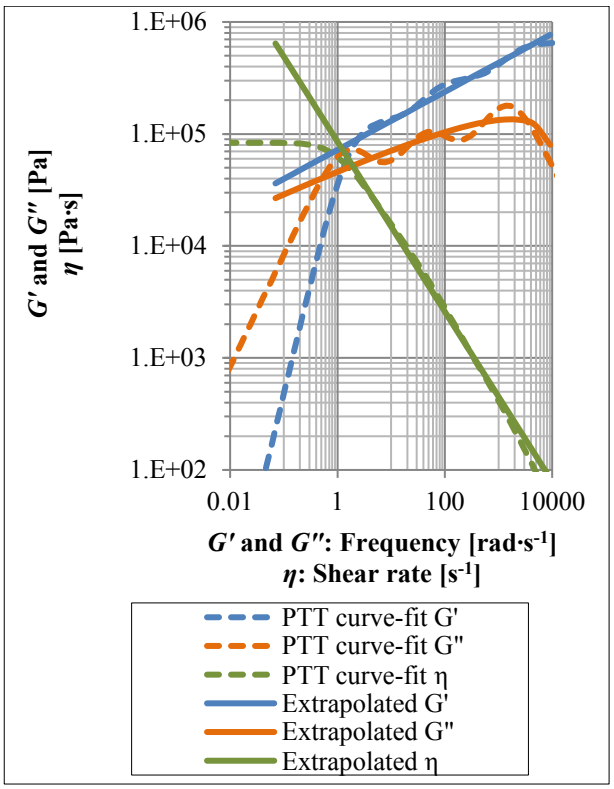

Figure 10: Extrapolated and curve fitted G', G" and η. Note: the dimensions differ between G', G'' and η. Note: all dimensions are presented on a logarithmic scale.

The typical shear rates range between 1 s^{-1} and 2000 s^{-1} as was determined with the trial simulation. Note that the fit matches well in the range of typical shear rates, but poorly at the shear rates of less than 1 s^{-1}.

Table 2: Curve-fitted values of the 3 mode PTT model. Note that there is only a single r for the multimode model, and that ε and ξ are identical for each mode.

	First mode	Second mode	Third mode
λ	$0.667 \cdot 10^{-3}$ s	$2 \cdot 10^{-3}$ s	0.6 s
η	230.803 Pa·s	3539.3 Pa·s	79880.5 Pa·s
ε	0.7508015	0.7508015	0.7508015
ξ	0.1360633	0.1360633	0.1360633
r	$0.41343 \cdot 10^{-6}$	-	-

Extrusion experiments

During the extrusion experiments the extrudate temperature and mass flow rate have been measured. Apollo tyres determined that the density of the rubber compound is 1210 $kg \cdot m^{-3}$.

Table 3: Measured flow rate and extrudate temperature for each experiment.

Gear pump speed	Flow rate	Extrudate temperature
5 rpm	13.9 $ml \cdot s^{-1}$	88 °C
10 rpm	27.4 $ml \cdot s^{-1}$	95 °C
15 rpm	41.1 $ml \cdot s^{-1}$	100 °C
20 rpm	54.2 $ml \cdot s^{-1}$	105 °C

The measured flow rates of Table 3 are used for the simulations.

Shear rates in the simulations

The simulations show high shear rates within the capillary part of the die. At higher flow rates the shear rates increase, but do not surpass 2130 s^{-1}. Which is in agreement with the typical shear rates found with the trial simulations and the chosen relaxation times.

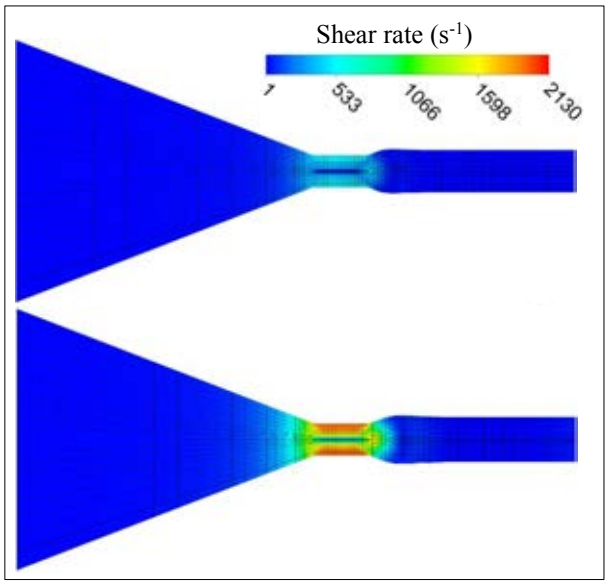

Figure 11: Shear rate in the extrudate swell simulations, upper diagram is 5 rpm, the lower diagram is 20 rpm.

Extrudate swell

The measured extrudate swell and the simulated extrudate swell are shown as a function of distance from the die exit:

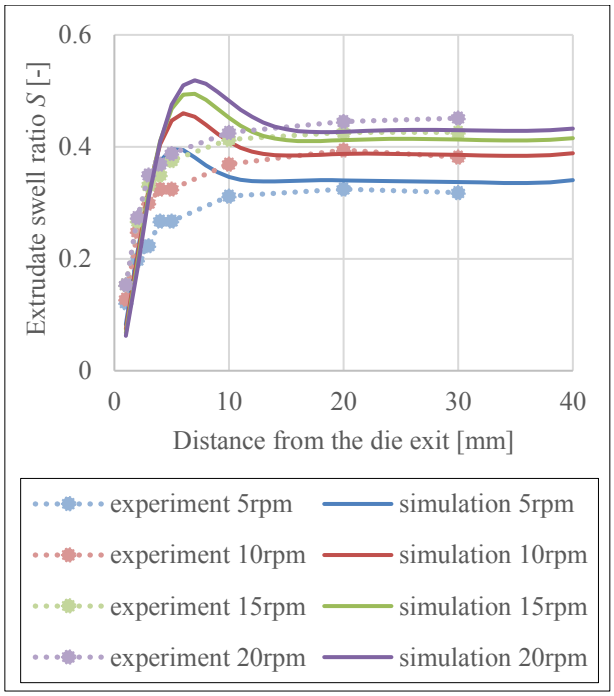

Figure 12: Experimental and simulated extrudate swell as a function of distance from the die exit, the legend shows the set gear pump speed of each experiment and simulation.

In these experiments the extrudate swell increases as a function of distance from the die exit up until 20 mm from the die exit. A small decrease in extrudate swell at

30 mm from the die exit can be observed. This is most likely a measurement error due to the downward curvature of the extrudate.
The simulations show a rapid increase in extrudate swell at a short distance from the die exit. The simulated extrudate swell seems to overshoot in comparison to the experiments. With more wall slippage, the overshoot disappeared.
The simulations show an increase of extrudate swell near the end of the 40 mm of simulated extrudate. This swell increases when the simulation is repeated with a shorter (20 mm) extrudate. A shorter extrudate has less time to relax. The extra swell near the end is most likely due to the boundary conditions at the outflow plane and the elastic tensions which have not completely been dissipated.
Figure 13 shows the simulated and experimental extrudate swell as a function of the flow rate at 20 mm from the die exit.

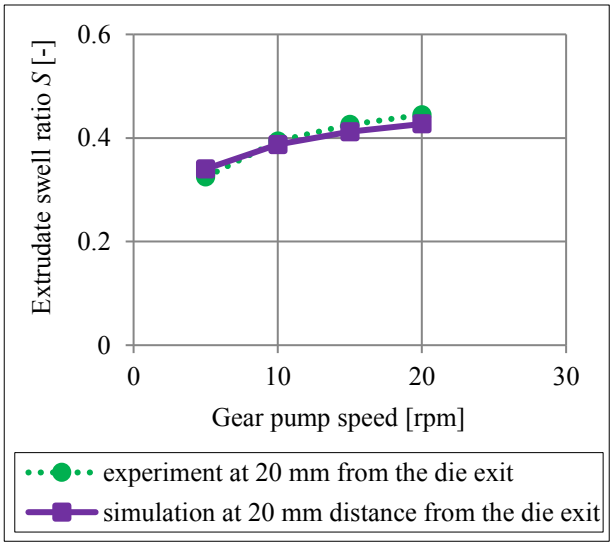

Figure 13: Experimental and simulated extrudate swell as a function of flow rate at 20 mm from the die exit.

There is strong agreement between the simulated and experimental extrudate swell. Both the simulated and experimental extrudate swell increase with higher flow rates, but the increase becomes less at higher flow rates.

CONCLUSION

A procedure was proposed to simulate extrudate swell. A rubber compound was analyzed for its rheological behavior and a 3 mode PTT model was fitted onto the rheological data. Extrudate simulations at high flow rates and shear rates have been performed with the PTT model. Extrusion experiments at high flow rates and shear rates have been performed. The extrudate swell was measured, the accuracy of the extrudate swell measurement is decreases beyond 30 mm from the die exit. The simulated swell is overpredicted near the die exit, the simulated swell and the experimental swell is in good agreement at 20 mm from the die exit.

Recommendations / Future work

The extrusion simulation was performed with a single circular die and a single tire rubber compound. Future work will focus on different die shapes and sizes, different tire compounds and different viscoelastic models.
In this study, rheological data was extrapolated. Further study is needed to determine whether the behavior of rubber matches the extrapolation.
Further research is needed to determine whether wall slippage is present in the die and how this might be included in the simulations. Wall slippage is not present at low shear rates, but might be present at high shear rates. The presence of wall slippage might be determined by experiments and simulations at low and high flow rates and shear rates. This could also be a validation of the simulation procedure at low flow rates.

ACKNOWLEDGEMENTS

This study was financially supported by Green Polymer Application Centre (Green PAC), Apollo tyres and VMI Group. The Windesheim University Professorship for Polymer Engineering conducted this study with project partners Apollo tyres, VMI Group and University of Twente. The project partners provided expert advice, essential equipment, materials and experimental data.

REFERENCES

1. Coelho, P.M., F.T. Pinho, and P.J. Oliveira, *Fully developed forced convection of the Phan-Thien–Tanner fluid in ducts with a constant wall temperature.* International Journal of Heat and Mass Transfer, 2002. **45**(7): p. 1413-1423.
2. Pittman, J.F.T., *Computer-aided design and optimization of profile extrusion dies for thermoplastics and rubber: a review.* Proceedings of the Institution of Mechanical Engineers, Part E: Journal of Process Mechanical Engineering, 2011. **225**(4): p. 280-321.
3. Thais, L., L. Helin, and G. Mompean, *Numerical simulation of viscoelastic flows with Oldroyd-B constitutive equations and novel algebraic stress models.* Journal of Non-Newtonian Fluid Mechanics, 2006. **140**(1-3): p. 145-158.
4. Debbaut, B. *Eureka project ID 2799: Development and industrial applications of explicity algebraic fluid models*. Available from: http://www.eurekanetwork.org/project/id/2799.
5. Choi, S.H. and M.Y. Lyu, *Application of the PTT Model for Capillary Extrusion of Rubber Compounds.* International Polymer Processing, 2009. **24**(4): p. 326-333.
6. *29th Annual Meeting and Conference on Tire Science and Technology*. 2010.
7. Ashutosh A. Kudale, K.N., G. Karthick Raja, P. Sankarganesh 2 , R. Rajesh Babu, *Extrusion Die Swell Simulation of Tire tread Compound using Phan Thien & Tanner (PTT) Model.*
8. Yang, C. and Z. Li, *Effects of wall slip on the rheological measurement and extrusion die design of a filled rubber compound.* Plastics, Rubber and Composites, 2016. **45**(7): p. 326-331.

9. Tanner, R.I., *Engineering rheology*. 1 ed. 1986: Oxford University Press.
10. Ahmed, R., R.F. Liang, and M.R. Mackley, *The experimental observation and numerical prediction of planar entry flow and die swell for molten polyethylenes.* Journal of Non-Newtonian Fluid Mechanics, 1995. **59**(2–3): p. 129-153.
11. Goublomme, A., B. Draily, and M.J. Crochet, *Numerical prediction of extrudate swell of a high-density polyethylene.* Journal of Non-Newtonian Fluid Mechanics, 1992. **44**: p. 171-195.
12. Goublomme, A. and M.J. Crochet, *Numerical prediction of extrudate swell of a high-density polyethylene: further results.* Journal of Non-Newtonian Fluid Mechanics, 1993. **47**: p. 281-287.
13. Konaganti, V.K., et al., *Extrudate Swell of High Density Polyethylenes in Slit (Flat) Dies.* International Polymer Processing, 2016. **31**(2): p. 262-272.
14. Konaganti, V.K., et al., *Extrudate swell of a high-density polyethylene melt: II. Modeling using integral and differential constitutive equations.* Journal of Non-Newtonian Fluid Mechanics, 2015. **225**: p. 94-105.
15. Ganvir, V., et al., *Extrudate swell of linear and branched polyethylenes: ALE simulations and comparison with experiments.* Journal of Non-Newtonian Fluid Mechanics, 2011. **166**(1-2): p. 12-24.
16. Kim, J.H. and M.Y. Lyu, *Predictions of flow behaviors and entrance pressure drop characteristics of a rubber compound in a capillary die using various rheological models.* Polymer Engineering & Science, 2014. **54**(10): p. 2441-2448.
17. Debbaut, B. and T. Marchal, *Numerical simulation of extrusion process and die design for industrial profile, using multimode pom–pom model.* Plastics, Rubber and Composites, 2008. **37**(2-4): p. 142-150.
18. Mompean, G., et al., *Numerical prediction of three-dimensional time-dependent viscoelastic extrudate swell using differential and algebraic models.* Computers & Fluids, 2011. **44**(1): p. 68-78.
19. Limtrakarn, W., et al., *Circular Die Swell Evaluation of LDPE Using Simplified Viscoelastic Model.* King Mongkut's University of Technology North Bangkok International Journal of Applied Science and Technology, 2013. **6**(3): p. 59-68.
20. Kim, J., et al., *Computer Simulation of Die Extrusion for Rubber Compound Using Simplified Viscoelastic Model.* Elastomers and Composites, 2011. **46**(1): p. 54-59.
21. Béraudo, C., et al., *A finite element method for computing the flow of multi-mode viscoelastic fluids: comparison with experiments.* Journal of Non-Newtonian Fluid Mechanics, 1998. **75**(1): p. 1-23.
22. Ganvir, V., et al. *Numerical and Experimental Studies on Extrudate Swell of Linear and Branched Polyethylenes*. in *TheXV International Congress onRheology, The Society ofRheology 80 Annual Meeting*. 2008. American Institute of Physics.
23. Ganvir, V., et al., *Prediction of extrudate swell in polymer melt extrusion using an Arbitrary Lagrangian Eulerian (ALE) based finite element method.* Journal of Non-Newtonian Fluid Mechanics, 2009. **156**(1-2): p. 21-28.
24. Mu, Y., et al., *Measurement and simulation of low-density polyethylene extrudate swell through a circular die.* Polymer International, 2009. **58**(5): p. 475-483.
25. Mu, Y., et al., *Finite-Element Simulation of Polymer Flow and Extrudate Swell Through Hollow Profile Extrusion Die with the Multimode Differential Viscoelastic Model.* Advances in Polymer Technology, 2013. **32**(S1): p. E1-E19.
26. Ganvir, V., et al., *Numerical and experimental studies on extrudate swell of branched polyethylene through axisymmetric and planar dies.* Journal of Polymer Engineering, 2011. **31**(2-3): p. 217-221.
27. Debbaut, B. and M.J. Crochet, *Further results on the flow of a viscoelastic fluid through an abrupt contraction.* Journal of Non-Newtonian Fluid Mechanics, 1986. **20**: p. 173-185.
28. Yang, C. and Z. Li, *An integrated numerical study of coextrusion flow inside and outside the die.* Journal of Applied Polymer Science, 2016. **133**(23).
29. Ren, Z., X.Y. Huang, and H.S. Liu, *3D Numerical study on the hollow profile polymer extrusion forming based on the gas-assisted technique.* IOP Conference Series: Materials Science and Engineering, 2016. **137**: p. 012007.
30. Pettas, D., et al., *On the origin of extrusion instabilities: Linear stability analysis of the viscoelastic die swell.* Journal of Non-Newtonian Fluid Mechanics, 2015. **224**: p. 61-77.
31. Konaganti, V.K., et al. *Study on extrudate swell of high-density polyethylenes in slit (flat) dies*. in *Annual Technical Conference - ANTEC, Conference Proceedings*. 2016.
32. Alpha-Technologies, *RPA2000*.
33. Macosko, C.W., *Rheology: Principles, Measurements, and Applications*. 1994: WILEY-VCH.
34. Owens, R.G. and T.N. Phillips, *Computational rheology*. 2002: World Scientific.
35. Konaganti, V.K., et al., *The effect of damping function on extrudate swell.* Journal of Non-Newtonian Fluid Mechanics, 2016. **236**: p. 73-82.
36. Konaganti, V.K., et al., *Non-isothermal extrudate swell.* Physics of Fluids, 2016. **28**(12).
37. ANSYS, *Polyflow manual.*
38. Leblanc, J.L., *Rubber-filler interactions and rheological properties in filled compounds.*

Progress in Polymer Science, 2002. **27**(4): p. 627-687.

39. Bhagawan, S.S., et al., *Effect of fillers on the rheological behavior of thermoplastic 1,2 polybutadiene rubber*. Polymer Engineering and Science, 1988. **28**(10): p. 648-654.

40. Yang, C. and Z. Li, *A study of wall slip in the capillary flow of a filled rubber compound.* Polymer Testing, 2014. **37**: p. 45-50.